Fusion of the LAPW and LMTO methods: The augmented plane wave plus muffin-tin orbital method

Takao Kotani
Department of Applied Mathematics and Physics, Tottori University, Tottori 680-8552, Japan

Mark van Schilfgaarde
School of Materials, Arizona State University, Tempe, Arizona 85284, USA

(Received 21 December 2009; revised manuscript received 26 February 2010; published 23 March 2010)

We present a full potential linearized method to solve the one-body problem, for example in the local density approximation. A mixed basis of augmented plane waves and generalized muffin-tin orbitals (MTOs) are used for the eigenfunctions. Since MTOs efficiently describe low-energy and localized states, the mixed basis is dramatically more efficient than the linearized augmented plane wave method for a given tolerance. GaAs, MnAs, $SrTiO_3$, Cu, and the O_2 dimer are used as illustrations.

DOI: 10.1103/PhysRevB.81.125117 PACS number(s): 71.15.Ap, 71.15.Nc, 71.15.Qe

Linear augmented-wave, full potential (FP) methods[1–3] are generally accepted to be the most accurate way to solve the effective single-particle Schrödinger equation (SE) encountered, for example, in the local density approximation. For their basis sets, methods such as the linearized augmented plane wave (LAPW) and the closely related projector augmented wave (PAW) method, and the method of linear muffin-tin orbitals (LMTOs), begin with a collection of envelope functions, which we denote here generally as $\{F^i\}$, and augment them in (muffin-tin) spheres centered around each nucleus with numerical wave functions, subject to matching at (or near) the sphere boundary.

Plane waves (PWs) are used for envelope functions in the LAPW and PAW methods. Owing to their facility to converge to the basis to any desired precision, they are usually the preferred choice. Atom-centered Hankel envelopes (which result in the LMTO method) are also widely used. LMTO is typically more efficient than LAPW because many orbitals (notably d states in transition metals and the $2s$ and $2p$ states in second-row atoms) are well localized and atomiclike. Thus we need to superpose many PWs to represent them well, while such states can be efficiently represented by the LMTO method, owing to its localized, real-space envelope functions. On the other hand, the LMTO method is thought to be less robust because there is no natural path to converging the basis to completeness. In this paper we present a scheme which integrates atom-centered and PW envelope functions, realizing in one approach advantages of the hitherto independent basis sets. We call this method the "plane-wave+muffin-tin orbital," or PMT method.

The two kinds of envelope functions can be fused in a natural way through a variant of the LMTO method developed recently.[4] This method differs from the usual one, first because efficient augmentation scheme makes it possible to choose many kinds of envelope functions in a simple, unified framework, as we briefly describe below. Moreover, the method of Ref. 4 adopts a different kind of atom-centered envelope function $\mathcal{H}_{\mathbf{R}L}$, namely the convolution of a Gaussian $g(r)=(\sqrt{\pi}r_s)^{-3}e^{-r^2/r_s^2}$, with a Hankel function H: viz $\mathcal{H}=g*H$. ($\mathbf{R}$ occurring in a subscript denotes where a function is centered, e.g., $\mathcal{H}_{\mathbf{R}L}(\mathbf{r})=\mathcal{H}_L(\mathbf{r}-\mathbf{R})$. $L=lm$ refers to the orbital quantum numbers, e.g., s,p,d functions.) In contradistinction to $H_{\mathbf{R}L}$ which diverges as $1/r^{l+1}$ for $r\to 0$, $\mathcal{H}_{\mathbf{R}L}$ is everywhere smooth: in particular $\mathcal{H}_{\mathbf{R}L}\propto r^l$ as $r\to 0$, and $\mathcal{H}_{\mathbf{R}L}\to H_{\mathbf{R}L}$ as $r\to\infty$.

Thus, the $\mathcal{H}_{\mathbf{R}L}$ are smooth while avoiding a well-known deficiency of Gaussian orbitals, namely, too-rapid asymptotic decay. "Smoothness" turns out to be very important for efficient evaluation of the Hamiltonian matrix elements, a key property the $H_{\mathbf{R}L}$ lack. Yet perhaps the most important, the $\mathcal{H}_{\mathbf{R}L}$ are a very efficient basis because they are better tailored to a molecular or crystal potential. The H_L solve the SE for a flat potential $V(\mathbf{r})=$const, since $(-\nabla^2-\epsilon)H_L(\epsilon,\mathbf{r})=0$, where in real systems the spherical part of $V(\mathbf{r})$ decreases when approaching a nucleus. Because the $\mathcal{H}_{\mathbf{R}L}$ satisfies $[-\nabla^2-\epsilon-4\pi\frac{G_L(r_s;r)}{\mathcal{H}_L(r_s,\epsilon;r)}]\mathcal{H}_L(r_s,\epsilon;\mathbf{r})=0$, where $G_L(\mathbf{r})=(\sqrt{\pi}r_s)^{-3}(\sqrt{2}/r_s)^{2l}e^{\varepsilon r_s^2/4-r^2/r_s^2}r^lY_L(\hat{\mathbf{r}})$, they can better adapt their shape to the true potential by tuning r_s.

Our augmentation procedure of Ref. 4 is a widely used standard procedure. It can be applied to our smooth envelope functions $F^i(\mathbf{r})$, which is a PW or a smoothed Hankel function $\mathcal{H}_{\mathbf{R}L}$, in the same manner. The method augments F^i in a MT sphere of radius $s_{\mathbf{R}}$ at point $\mathbf{R}$, by "augmenting" its one-center expansion, $F^i(\mathbf{r})\equiv\Sigma_L F^i_{\mathbf{R}L}(\mathbf{r})$, with a linear combination of numerical solutions of the SE, $\Sigma_L\tilde{F}^i_{\mathbf{R}L}(\mathbf{r})$. In the linear theory, a radial solution $\phi_{Rl}(\varepsilon_{Rl},r)$ of the SE and its energy derivative, $\dot{\phi}_{Rl}(\varepsilon_{RL},r)$, are calculated for a given $\mathbf{R}l$, and $\tilde{F}^i_{\mathbf{R}L}$ is constructed out of the linear combination that matches value and slope of $F^i_{\mathbf{R}L}$ at $s_{\mathbf{R}}$. Thus the basis function reads

$$\tilde{F}^i(\mathbf{r})=F^i(\mathbf{r})+\sum_{\mathbf{R}L}\tilde{F}^i_{\mathbf{R}L}(\mathbf{r})-F^i_{\mathbf{R}L}(\mathbf{r}). \quad (1)$$

Ref. 4 calculates matrix elements of a $\langle\tilde{F}^i|\hat{O}|\tilde{F}^j\rangle$ of an operator $\hat{O}$ through the following:

$$\langle\tilde{F}^i|\hat{O}|\tilde{F}^j\rangle=\int d^3rF^{i^*}(\mathbf{r})\hat{O}F^j(\mathbf{r})+\sum_{\mathbf{R}}\int_{r<s_{\mathbf{R}}}d^3r[\tilde{F}^{i*}_{\mathbf{R}L}\hat{O}\tilde{F}^j_{\mathbf{R}L'}-F^{i*}_{\mathbf{R}L}\hat{O}F^j_{\mathbf{R}L'}]. \quad (2)$$

The interstitial integral (first term) is evaluated through all space; then the local parts are projected out.[5] Equation (2) is distinct from conventional augmentation: integrals are not evaluated by straightforward substitution of Eq. (1) which would entail cross terms, e.g., $\int_{r<s_{\mathbf{R}}} d^3 r \tilde{F}^{i*}_{\mathbf{R}L} \hat{O} F^j_{RL'}$. It is similar to a construction first developed by Soler and Williams.[2,6] It works well because the local term $\tilde{F}^{i*}_{\mathbf{R}L} \hat{O} \tilde{F}^j_{RL'} - F^{i*}_{\mathbf{R}L} \hat{O} F^j_{RL'}$ vanishes in both value and slope as $r \to s_{\mathbf{R}}$; the information in this region is carried entirely by the unaugmented part $F^{i^*}(\mathbf{r}) \hat{O} F^j(\mathbf{r})$. The local part turns on smoothly and becomes non-negligible only for r significantly smaller than $s_{\mathbf{R}}$. Since high L partial waves contribute predominantly in the region $r \to s_{\mathbf{R}}$, this scheme has a very rapid L convergence (typically $2 \le l_{\max} \le 4$).[4] It is this fact that makes augmentation so efficient and explains why pseudopotentials can be truncated to very low l cutoff while conventional augmented-wave methods require $6 \le l_{\max} \le 8$ for a comparable precision.

Finally, we outline a prescription for the one-center expansion. Instead of using standard functions, e.g., Bessel functions for PWs or $H_{\mathbf{R}L}$, the method of Ref. 4 adopts polynomials $P_{kL}(\mathbf{r})$, viz

$$\tilde{F}^i(\mathbf{r}) = F^i(\mathbf{r}) + \sum_{\mathbf{R}kL} C^{(i)}_{\mathbf{R}kL} \{ \tilde{P}_{\mathbf{R}kL}(\mathbf{r}) - P_{\mathbf{R}kL}(\mathbf{r}) \}. \tag{3}$$

P_{kL} are related to the generalized Laguerre polynomials,

$$P_{kL}(\mathbf{r}) = \frac{(-2)^k k! (2l+1)!!}{(2k+2l+1)!!} L_k^{l+1/2}\left(\frac{r^2}{r_s^2}\right) \frac{r^l}{r_s^l} Y_L(\hat{\mathbf{r}}), \tag{4}$$

and $\tilde{P}_{kL}$ are linear combinations of (ϕ and $\dot{\phi}$) that match value and slope of P_{kL} at $s_{\mathbf{R}}$. Owing to the orthogonality relation

$$\int_0^\infty dz e^{-u} u^{l+1/2} L_k^{l+1/2}(u) L_{k'}^{l+1/2}(u) = \frac{\Gamma\left(k+l+\frac{3}{2}\right)}{2k!} \delta_{kk'}, \tag{5}$$

any given function $f(r)$ for $0 \le r < \infty$ can be expanded as

$$f(r) = \frac{2k!}{\Gamma\left(k+l+\frac{3}{2}\right)} \sum_k c_{kL}(r_s) L_k^{l+1/2}(r^2/r_s^2). \tag{6}$$

Here the coefficients $c_{kL}(r_s)$ are determined from Eq. (5). With this expansion applied to radial functions for each L channel, we can have a following expansion for any function $F(\mathbf{r})$ as

$$F(\mathbf{r}) = \sum_L f_L(r) r^l Y_L(\hat{\mathbf{r}}). \tag{7}$$

See Ref. 8 (especially Sec. XII) for explicit expressions for PWs, smoothed Hankels $\mathcal{H}_L$ and many other useful properties of an interesting class of functions, of which the $\mathcal{H}_L$ are members. Efficient augmentation for any shaped $F(\mathbf{r})$ depends only on whether analytic expressions for Eq. (7) can be obtained. Adapting the method of Ref. 4 to different $\{F^i\}$ entails little more than coding expressions for $C^{(i)}_{\mathbf{R}kL}$ specific to them. PWs, Gaussians, $\mathcal{H}_{\mathbf{R}L}$, and any number of envelope functions can be expanded with equal ease in the single, unified framework of Ref 4. Expressions for total energy, forces, assembling output density, etc., remain unchanged.

Our method has three distinct kinds of orbitals: APWs, smoothed LMTOs, and local orbitals. With a standard linear method, an eigenfunction will approximate the exact wave function for partial wave Rl by the linear combination $\phi_{Rl}(\varepsilon_{RL}, r) + \dot{\phi}_{Rl}(\varepsilon_{RL}, r)(\varepsilon - \varepsilon_{RL})$, i.e., a solution to the SE exact (for the spherical part of the potential) to linear order in $\phi_{Rl}(\varepsilon, r)$ around the linearization energy ε_{RL}. A great triumph of the linear method is that ϕ_l tends to be a smooth function of energy, so the Taylor series is rapidly convergent. Still, there are cases where the Taylor series is not sufficient for certain l partial waves, e.g., the Ga d channel. (This is particularly true in the GW context[7,9]). In this method, a local orbital can be added, which consists of a radial solution $\phi^z_{Rl}(r)$ to the SE at a different energy. For deep states, a smooth Hankel is attached which extends $\phi^z_{Rl}(r)$ into the interstitial while matching value, slope, and laplacian at $s_{\mathbf{R}}$. This kind of local orbital is very close to an eigenstate of any deep state without requiring other basis functions. The local orbitals we use are described in more detail in Ref. 7.

In Fig. 1 we present convergence studies for three representative crystals (GaAs, ferromagnetic MnAs, $SrTiO_3$) and the O_2 dimer. We selected four groups of localized basis sets, which consist of some materials-specific combination of smoothed LMTO's and local orbitals. We classify them into: (1) the "null' basis (consisting of some local orbitals but no LMTOs), (2) a "hyperminimal" basis (consisting of enough LMTOs to describe the valence band but little else), (3) a "small" basis (a standard minimum-basis LMTO calculation when accuracy is not important), and (4) a "large" basis—a typical LMTO basis for standard calculations. Table I presents their orbital characters for each material.

Particularly when the MTO and APW basis sets are both sizable, the PMT basis suffers from strong linear dependency. This is because that some MTO basis functions can be almost completely constructed as linear combinations of APWs; this means that when many MTOs and APWs are simultaneously included, the basis becomes overcomplete and linear dependency unacceptably large. For normally acceptable tolerances in convergence, this is not usually an issue. However for highly converged basis sets, it is necessary to remove the linear dependence. This can be largely accomplished by diagonalizing the overlap matrix, and reducing the Hilbert space to the subspace spanned by eigenfunctions whose overlap eigenvalues exceed a minimum tolerance (typically 10^{-6}). An extreme case is Cu: combining the large basis (Table I) with APWs up to an energy cutoff $E^{\mathrm{APW}}_{\mathrm{MAX}}$=400 eV (Fig. 2), the rank of the secular matrix was reduced from 272 to 237.[11] When the basis becomes very large, even the subspace projection occasionally has slight problems with stability. Little change is seen, for example, in the last and second-last small basis points for MnAs because of this. Note that the diagonalization of overlap matrix should be not necessary for practical usage to treat large systems because MTOs are sufficiently linearly independently when we use not so many APWs, or we can remove some MTOs (e.g., MTO for Sr 5s) in advance so that we do not need to remove some basis by diagonalization of the overlap.

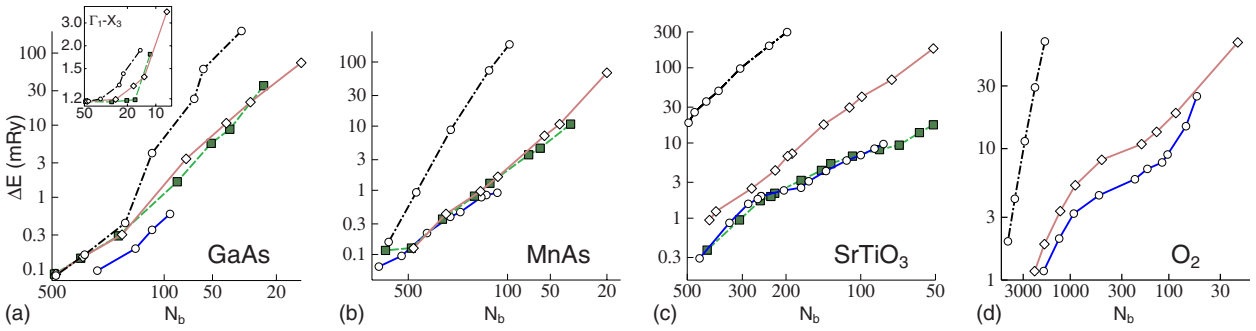

FIG. 1. (Color online) Deviation ΔE from fully converged total energy/atom, in mRy vs total number of basis functions N_b^Γ at Γ. Data are drawn on a log ΔE−log $1/N_b^\Gamma$ scale. Each curve corresponds to a fixed MTO+local orbital basis (see Table I). The basis is enlarged by increasing the PW energy cutoff E_{MAX}^{APW}. Data is shown for three periodic crystals and the O_2 dimer. Dashed-dot lines with circles are the closest to a pure LAPW basis (null in Table I); solid lines with diamonds correspond to the hyperminimal LMTO basis in Table I; dashed lines with squares employ a minimal LMTO set (small in Table I); finally, solid lines with circles contain the most LMTO's (large in Table I), corresponding to a standard LMTO calculation. The rightmost points in the minimal and large basis set cases correspond to all-LMTO basis sets. GaAs panel inset: Γ_1-X_3 transition between the conduction band minimum and second conduction band at X. (The large basis is not shown because it is converged to <0.01 eV without APWs.)

Figure 1 shows the deviation ΔE in total energy relative to the fully converged result as a function of the secular matrix dimension at Γ, N_b^Γ.[10] For the most part, fewer total functions are required to achieve a given accuracy when more LMTOs are used. On the other hand, the difficulty LMTO basis sets suffer in controlling convergence to arbitrarily high precision is also apparent. These pictures neatly highlight the respective advantages of both LAPW and LMTO methods; they also show clearly that a union of the two combines the respective advantages. The reduction in basis dimension by augmenting LAPWs with at least some LMTO set is dramatic. The four cases of Fig. 1 show that the

TABLE I. The null, "hyperminimal," small, and large LMTO+Local orbital (LO) basis sets for GaAs, MnAs, $SrTiO_3$, the O_2 dimer, and Cu. Column "Float" signifies MTO's centered in interstitial regions. Column N indicates the total number of orbitals excluding APWs. The large basis set in the GaAs case is one used in Ref. 7.

Basis	LMTO			LO			N
	Ga	As	Float	Ga	As		
Null				3*d*	4*s*		6
Hyper	*sp*	*sp*		3*d*	4*s*		14
Small	*spd*	*spd*		3*d*	4*s*		24
Large	*spdfg*,*spd*	*spdfg*,*spd*	*spdspd*	3*d*	4*s*		92
	Mn	As		Mn	As		
Null							0
Hyper	*sd*	*sp*					20
Small	*spd*	*spd*					36
Large	*spdf*,*spd*	*spdf*,*spd*					100
	Sr	Ti	O	Sr	Ti	O	
Null				3*p*	3*p*		6
Hyper			*sp*	3*p*	3*p*		18
Small	*spd*	*spd*	*spd*	3*p*	3*p*		51
Large	*spdsp*,*sp*	*spd*,*spd*	*spdsp*	3*p*	3*p*		81
		O			O		
Null					2*s*		2
Hyper		*sp*					20
Large		*spdf*,*spd*			3*s*		52
		Cu			Cu		
Null					5*s*, 5*p*, 4*d*		9
Large		*spdfg*,*spd*			5*s*, 5*p*, 4*d*		43

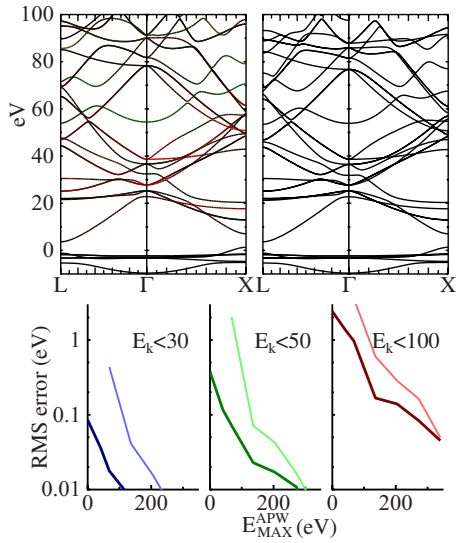

FIG. 2. (Color online) Energy bands for Cu, in eV. Fermi level at zero. Top left: large LMTO basis of Table I, without APWs. Red depicts 4*d* orbital character, significant between 25 and 50 eV; green depicts 5*sp* orbital character. The state near 55 eV at Γ is mostly Cu 5*s*. Top right: converged 'large' basis with APWs. Bottom figures show RMS deviation (eV) relative to fully converged (Ref. 10) bands as a function of the PW cutoff energy $E_{\mathrm{MAX}}^{\mathrm{APW}}$, in the following energy windows: (left) $-10<E_k<30$ eV; (middle) $-10<E_k<50$ eV; (right) $-10<E_k<100$ eV. Light lines: null basis of Table I; dark lines: large basis.

"optimal" partitioning between MTOs and LAPWs depends somewhat on the case. We can make the following observations:

(i) when moderate accuracy is sought (~3 mRy/atom), a standard LMTO basis can converge the total energy with vastly fewer orbitals than a standard LAPW basis, the ratio of orbitals for a fixed precision being on the order of 5. Compare the null case to the other cases in Fig. 1.

(ii) It can be difficult to converge a standard LMTO basis to high accuracy, e.g., <1 mRy/atom; see in particular the rightmost point on the dashed-line-with-squares and solid-line-with-circles curves in $SrTiO_3$ and O_2, Fig. 1.

(iii) When high accuracy is required, a certain number of MTOs can dramatically improve convergence. Once a certain number of LMTOs is included (the number and kind depending on the material), it often makes little difference whether more LMTOs or LAPWs are added. This is true to the extent that curves overlap in Fig. 1. In the absence of any advantage gained by using LMTOs, LAPWs are preferred since they are easier to define and construct.

Perhaps the most surprising and dramatic results are those for O_2. Even the *spdf-spd* atom-centered basis is rather poorly converged in the total energy. Standard localized basis sets used in the quantum chemical community do better, as do LMTO basis sets with more than two radial functions per *l*.[12] On the other hand, the 'null' APW+2*s*(LO) basis requires a large number of APWs to converge ΔE to acceptable tolerances.

It would be interesting to compare these results using *optimally chosen* real-space basis sets. Near-optimal real-space basis sets have been constructed within the framework of "shape-approximate" (i.e., superposition of spherical) potentials.[13] Such basis sets permit a marked reduction in the size of the secular matrix compared to functions used here, for a fixed accuracy. However, (near) optimal basis sets have never been designed for a full potential method, so such a comparison is not possible today. In any case, it seems to be generally true that the fusion of a local basis with an APW basis dramatically reduces the required size of the secular matrix relative to the LAPW method and offers a systematic path to arbitrarily high accuracy starting from the LMTO method.

Derivative properties of the total energy, e.g., lattice constant *a*, magnetic moment *M*, the bulk modulus *B*, and other shear moduli, are less sensitive to details of the basis than the total energy itself. *a* and *B* are already rather well converged in each material using small MTO sets of Table I. Ref. 14 tabulates well converged LAPW results for the cohesive energy E_{coh}, *a* and *B* in GaAs: $E_{coh}=0.587$ Ry, $a=10.62$ a.u., $B=74$ GPa. Our results are similar: $E_{coh}=0.575$ Ry, $a=10.61$ a.u., $B=75$ GPa. We do not believe that the small difference in E_{coh} can be attributed to incomplete basis convergence in either case, but to other factors.[10] Our results for Cu ($a=6.65$ a.u., $B=187$ GPa) are also very similar to an LAPW calculation[15] ($a=6.65$ a.u., $B=192$ GPa).

The LAPW basis is especially well suited for high-energy states. Reliable description of such states is important for some optical properties; they can be important when computing the RPA total energy.[16] The LMTO method describes lower unoccupied states very well but its accuracy degrades with increasing energy. An instructive example is Cu (Fig. 2), because the 4*d* partial waves are important above 25 eV: states near Γ 27 and 39 eV are largely of 4*d* character. At higher energies, the 5*s* partial wave is important; see particularly the state at ~55 eV near Γ. In a strictly linear method these states are wrongly placed, by ~5 eV. Accordingly our basis contains 5*s*, 5*p*, and 4*d* LOs. We consider two cases: a null basis of APW+LOs, and a large basis augmented by LMTOs (Table I). The top panels of Fig. 2 compare the large, APW-free basis ($E_{\mathrm{MAX}}^{\mathrm{APW}}=0$) to a highly converged basis. Differences begin to become apparent to the eye above 50 eV. The bottom panels quantify the RMS deviation in the bands (computed relative to a well converged basis) for both the 'null' and the large basis. These panels show that the fused MTO and APW basis converges wrt $E_{\mathrm{MAX}}^{\mathrm{APW}}$ dramatically faster than APWs alone (the advantage disappears for small RMS deviations in high-lying bands). Another revealing example because it is slow to converge, is the transition between the conduction band minimum at Γ and the second conduction band at *X* in GaAs. Convergence is shown in the inset of the top left panel of Fig. 1. Addition of a small LMTO basis dramatically reduces the required number of APWs basis for a given convergence.

To summarize, we show how a fused basis of APWs and MTOs based on smoothed Hankel functions combines advantages of the LAPW and MTO basis sets, in a single very accurate and efficient scheme.

This work was supported by ONR Contract No. N00014-7-1-0479 and NSF Grant No. QMHP-0802216.

[1] O. K. Andersen, Phys. Rev. B **12**, 3060 (1975).
[2] J. M. Soler and A. R. Williams, Phys. Rev. B **40**, 1560 (1989).
[3] P. E. Blöchl, Phys. Rev. B **50**, 17953 (1994).
[4] M. Methfessel, M. van Schilfgaarde, and R. A. Casali, in *Lecture Notes in Physics*, edited by H. Dreysse (Springer-Verlag, Berlin, 2000), Vol. 535.
[5] There are some subtleties when the operator is the one-body potential; see Ref. 4.
[6] The PAW method[3] uses a similar construction. It is the one of primary differences between PAW and conventional LAPW.
[7] M. van Schilfgaarde, T. Kotani, and S. V. Faleev, Phys. Rev. B **74**, 245125 (2006).
[8] E. Bott, M. Methfessel, W. Krabs, and P. C. Schmidt, J. Math. Phys. **39**, 3393 (1998).
[9] S. V. Faleev, M. van Schilfgaarde, and T. Kotani, Phys. Rev. Lett. **93**, 126406 (2004).
[10] By "fully converged" we do not mean absolute convergence, but convergence for the given Hilbert space of ϕ_{Rl}, $\dot{\phi}_{Rl}$, and ϕ^z_{Rl}, finite l cutoff in augmentation and within the frozen core approximation where the core tails are expanded into the interstitial by attaching a smoothed Hankel function.
[11] A drawback of this procedure is that slight discontinuities arise, e.g., in the k dependence of the energy bands or the total energy vs lattice constant.
[12] M. Methfessel, M. van Schilfgaarde, and M. Scheffler, Phys. Rev. Lett. **70**, 29 (1993).
[13] O. K. Andersen, T. Saha-Dasgupta, R. W. Tank, C. Arcangeli, O. Jepsen, and G. Krier, in *Lecture Notes in Physics*, edited by H. Dreysse (Springer-Verlag, Berlin, 2000), Vol. 535.
[14] C. Filippi, D. J. Singh, and C. J. Umrigar, Phys. Rev. B **50**, 14947 (1994).
[15] A. Khein, D. J. Singh, and C. J. Umrigar, Phys. Rev. B **51**, 4105 (1995).
[16] T. Miyake, F. Aryasetiawan, T. Kotani, M. van Schilfgaarde, M. Usuda, and K. Terakura, Phys. Rev. B **66**, 245103 (2002).